Analytical Methods

Cite this: *Anal. Methods*, 2012, **4**, 1729

www.rsc.org/methods

PAPER

A highly selective and sensitive pyridylazo-2-naphthol-poly(acrylic acid) functionalized electrospun nanofiber fluorescence "turn-off" chemosensory system for Ni^{2+}

Sheriff Adewuyi, Dezzline A. Ondigo, Ruphino Zugle, Zenixole Tshentu, Tebello Nyokong and Nelson Torto*

Received 20th February 2012, Accepted 22nd March 2012
DOI: 10.1039/c2ay25182e

A fluorescent nanofiber probe for the determination of Ni^{2+} was developed *via* the electrospinning of a covalently functionalized pyridylazo-2-naphthol-poly(acrylic acid) polymer. Fluorescent nanofibers with diameters in the range 230–800 nm were produced with uniformly dispersed fluorophores. The excitation and emission fluorescence were at wavelengths 479 and 557 nm respectively, thereby exhibiting a good Stokes' shift. This Ni^{2+} probe that employs fluorescence quenching in a solid receptor–fluorophore system exhibited a good correlation between the fluorescence intensity and nickel concentration up to 1.0 μg mL^{-1} based on the Stern–Volmer mechanism. The probe achieved a detection limit (3δ/S) of 0.07 ng mL^{-1} and a precision, calculated as a relative standard deviation (RSD) of <4% ($n = 8$). The concentration of Ni^{2+} in a certified reference material (SEP-3) was found to be 0.8986 μg mL^{-1}, which is significantly comparable with the certified value of 0.8980 μg mL^{-1}. The accuracy of the determinations, expressed as a relative error between the certified and the observed values of certified reference groundwater was ≤0.1%. The versatility of the nanofiber probe was demonstrated by affording simple, rapid and selective detection of Ni^{2+} in the presence of other competing metal ions by direct analysis, without employing any further sample handling steps.

Introduction

In recent years a great deal of research has been devoted to the detection of metal ions in environmental or biological systems.[1] Nickel is an essential metal for supporting life, as loss of nickel homeostasis is harmful to prokaryotic and eukaryotic organisms alike.[2] Although the contributions of nickel homeostasis to mammalian health and diseases remain largely unexplored,[3] excess nickel accumulation can aberrantly affect respiratory and immune systems.[4,5] Therefore, it is very important to detect nickel ions. Advances in both electronics and mechanics have yielded high-tech facilities that are widely available for the detection of nickel metal ions at low concentration levels (0.1 ng mL^{-1}),[6] for example, techniques such as inductively coupled plasma-optical emission spectrometry (ICP-OES),[7,8] microwave-induced plasma (MIP),[9] electrothermal atomic absorption spectrometry (ETAAS),[10–12] flame atomic absorption spectrometry (FAAS),[13,14] spectrophotometry,[15,16] voltammetry and inductively coupled plasma-mass spectrometry (ICP-MS).[17] Some of these methods are complicated and are not suitable for quick and on-line monitoring. In this regard, the fluorescence methods remain the most favorable options due to their advantages over other techniques, which include ease of detection, sensitivity and instantaneous response.[18–24]

In fluorescence techniques, suitable indicators which are sensitive to analyte concentrations and exhibit changes in fluorescence intensity are used as molecular recognition materials.[25] Recently, derivatives of 8-hydroxyquinoline were used as sensitive and reliable tools to measure concentrations and fluctuations of cellular Mg^{2+} by comparing the enhancement of the fluorescence with analyte concentrations.[26] Also, boradiazaindacene as the fluorophore with 4-(bis(pyridin-2-ylmethyl)amino)-benzaldehyde was employed for an intracellular emission fluorescent Cd^{2+} sensor based on the internal charge transfer (ICT) mechanism.[27,28] Other examples involve a fluorescence response system with poly[*p*-(phenyleneethynylene)-*alt*-(thienyleneethynylene)]. It showed varying fluorescence "turn-on" behavior in the presence of cations including Li^+, Na^+, K^+, Mg^{2+}, Ca^{2+}, H^+, Mn^{2+}, Fe^{2+}, Co^{2+}, Ni^{2+}, Zn^{2+}, Cd^{2+} and Hg^{2+}.[22] Most of these literature reports involve the use of fluorescent sensors in liquid rather than in solid state.

Successively, exploration of well defined fluorescence "turn-off" indicators with a large Stoke shift, high quantum yield, strong absorbance, excellent photostability and non-toxicity will be of high interest for research. Fluorophores for heavy metals take advantage of the high affinity of oxygen and nitrogen donor atoms towards these ions according to the principles of hard or soft bases and acids (HSAB) by Pearson.[29] An example of such

Department of Chemistry, Rhodes University, P.O. Box 94, Grahamstown, 6140, South Africa. E-mail: N.Torto@ru.ac.za

an indicator with complexing preference for a borderline acid like Ni^{2+} is 1-(2-pyridylazo)-2-naphthol (PAN); more so it is one of the most sensitive reagents among heterocyclic azo compounds for determining heavy metals.[30] In order to confer some special properties, organic and inorganic polymers have been used as solid supports for the fluorescence indicators. It is known that the choice of solid supports and the immobilization of indicators into the supports have significant effects on the performance of the sensors in terms of selectivity, sensitivity, response time, and stability.[31,32] Most importantly, it will afford electrospinable material for transformation into a nanofiber mat for solid phase measurement.

Electrospinning of polymeric materials into well-defined fiber mats has received significant interest due to their potential for a variety of applications. Specifically, the technique has been found to be a unique and cost-effective approach for fabricating large surface area membranes for a variety of sensor applications.[33–38] Previously, Wang *et al.* had shown that the sensitivities of the electrospun nanofiber to detect Fe^{3+} and Hg^{2+} are 2 to 3 orders of magnitude higher than those obtained from thin film sensors.[33] Since new methods are emerging for the development of highly sensitive solid-state detectors of heavy and transition metal ions using fluorescence spectroscopy,[39–43] it is expected that electrospun polymers featuring fluorescence indicators could exhibit amplified fluorescence "turn-off" effects when the complexing units bind to metal ions.

The indicators are immobilized by physical or chemical procedures onto the polymeric materials.[31] The physical procedures used for immobilization include adsorption,[44–46] dissolution,[47,48] entrapment in a porous network[49,50] and ion exchange.[51] These methods are simple but suffer from the limitation of insolubility of the indicator in the polymeric support, which results in leaching out of the indicator. The chemical procedure involves the formation of covalent bonds between the indicator and support materials. Sensors with covalently immobilized indicators have the advantage of not suffering from indicator leach-out.[52,53] Therefore, considering the importance of detecting Ni^{2+} in the environment, this contribution focused on the functionalization of PAN into an optimally selected polymer such as poly(acrylic acid) (PAA) by a simple esterification procedure (Scheme 1) to yield a fluorescence polymer PAN–PAA. The functionalized polymer was further electrospun into a nanofiber mat to obtain the fluorescence "turn-off" chemosensory system as a highly selective and sensitive detector of Ni^{2+} in an aqueous solution. Detailed investigations and results are herein reported.

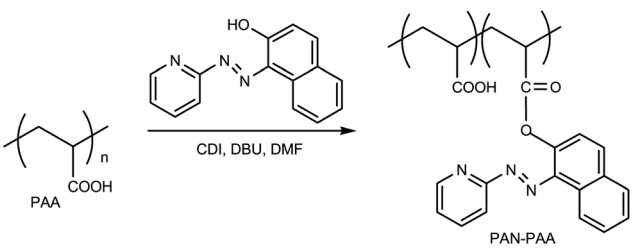

Scheme 1 Fluorescence functionalized polymer of 1-(2-pyridylazo)-2-naphthol and poly(acrylic acid) (PAN–PAA).

Experimental section

Materials and reagents

All experimental manipulations and data collections were performed at room temperature, unless otherwise stated. PAA (M_w = 50 000 g mol^{-1}), PAN, 1,1′-carbonyldiimidazole (CDI), 1,8-diazabicyclo[5.4.0]undec-7-ene (DBU) and all inorganic salts ($NiCl_2 \cdot 6H_2O$, $CoCl_2 \cdot 6H_2O$, $CrCl_3 \cdot 6H_2O$, $CuCl_2 \cdot 6H_2O$, $FeSO_4 \cdot 7H_2O$, $Cd(NO_3)_2 \cdot 4H_2O$, $Zn(NO_3)_2 \cdot H_2O$, $Pb(NO_3)_2$ and $Al_2(SO_4)_3 \cdot 15H_2O$) were of analytical grade and were used as obtained from Sigma Aldrich (St Louis, USA). *N*,*N*-Dimethylformamide was purchased from Merck Chemicals (Wadesville, South Africa) and distilled over nitrogen at reduced pressure. Standard solutions were freshly prepared by dissolving known quantities of metal salts in deionized ultrapure water obtained from a Millipore system.

Synthesis of fluorescence polymer (PAN–PAA)

A solution of CDI (0.34 g, 2.1 mmol) and a catalytic amount of DBU in 10 mL of dimethylformamide (DMF) were added to a solution of PAA (1.5 g, 20.8 mmol) in 40 mL of DMF. After stirring the solution at 70 °C until the evolution of carbon dioxide subsided (15 min), a solution of PAN (0.52 g, 2.08 mmol) in 15 mL DMF was added and the solution was stirred at 70 °C for 18 h. The solution was slowly transferred with vigorous stirring into diethyl ether to precipitate the polymer. After filtration, the obtained solid was washed extensively with ether and acetone and dried in a vacuum oven for 24 h at 25 °C.

Fabrication of fluorescence electrospun nanofiber

A solution for electrospinning was prepared by dissolving 6.6 wt% PAN–PAA in 1 : 4 (v/v) water–ethanol solvent system and stirred overnight to obtain a homogeneous solution. After loading the polymer solution into a 10 mL glass syringe, the syringe was mounted on a programmable syringe pump (New Era, NE-1000). The solution was pumped at a flow rate of 1 mL h^{-1} through a steel needle of internal diameter 0.584 mm. Nanofibers were collected on glass slides which were covered with masking tape and only the targeted area (0.5 × 2.5 cm) exposed for deposition to occur. This system was mounted on aluminium foil and the collection was carried out in 8 min. The distance between the needle tip and the collector was 15 cm and the voltage applied at the needle tip was 8.75 kV. In order to improve the insolubility of the fiber mat in an aqueous medium, the electrospinning solution with cross-linker was prepared with the addition of β-cyclodextrin at 20 wt% of the product. After the deposition process, fibers were heat treated at 120 °C for 20 min to cross-link the films.

Characterization

Infrared spectra were recorded on a Perkin-Elmer 100 FT-IR spectrophotometer. Electronic absorption spectra were recorded on a Perkin-Elmer Lambda 25 UV/VIS spectrophotometer in a quartz cell (1 cm). Emission spectra were recorded on a Varian Cary Eclipse spectrofluorometer in a 1 cm quartz cell. The spectrofluorometer was equipped with a xenon discharge lamp

(75 kV), Czerny–Turner monochromators and an R-928 photomultiplier tube with a manual or automatic voltage that was controlled using the Cary-Eclipse software. All samples were illuminated at an excitation wavelength of 500 nm and the emission was scanned from 510 to 640 nm, while the detector voltage was maintained between 600 and 650 V. The morphology of the nanofiber mat was studied by the Tescan (TS5136ML) Scanning Electron Microscope (SEM) operating at an accelerated voltage of 20 kV after a gold sputter coating. The fluorescence images were taken with a DMLS fluorescence microscope. The excitation source was a high-voltage mercury lamp and light with a wavelength of around 470–570 nm was emitted with the help of an optical filter. The exposure time was the same for all images.

Fluorescence measurements

In order to perform fluorescence measurements, the glass slides containing sensor layers (Fig. 1) were placed in a 1 cm quartz cuvette which was filled with various metal salt solutions. The cuvette was placed in the sample holder of the spectrofluorometer, samples were illuminated at an excitation wavelength of 500 nm and the emission was scanned from 510 to 640 nm, while the detector voltage was maintained between 600 and 650 V.

Fluorescence quenching detection of Ni^{2+} by electrospun nanofiber

In fluorescence data collection, the 5 mL aliquots of nickel ion stock solutions (range 0.1–1.0 μg mL^{-1}) were added into an optical cell containing a glass slide coated with the sensing nanofiber. Upon introducing series of the nickel ion solutions, fluorescence quenching of the sensing nanofiber was observed. The data, corresponding to the average of three determinations, were fitted by a standard least-squares treatment and the Stern–Volmer equations were evaluated. The procedure for examining the influence of other metal ions on the fluorescence quenching of Ni^{2+} was essentially the same. In this case, the sensing nanofiber was exposed to several metal cations at higher equivalence with or without a fixed concentration of nickel ions. A custom-made certified reference material for groundwater (SEP-3) purchased from Inorganic Ventures (Christiansburg, USA) was used to validate the analytical procedure. The repeatability of the method was evaluated by comparing the signals obtained from three determinations of the reference material.

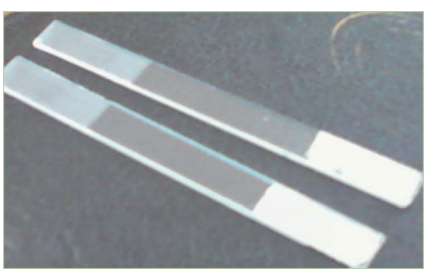

Fig. 1 Photograph of glass slides coated with fluorescent nanofibers.

Results and discussion

Fabrication and characterization of fluorescence PAN–PAA nanofiber

PAN has been shown to be one of the most sensitive reagents among heterocyclic azo compounds for determining nickel ion.[25,30] FTIR spectra shown in Fig. 2 indicate a new ester bond formation (ν = 1737.07 cm^{-1}) between the hydroxyl groups of PAN and carboxylate groups of PAA. The formation of the new covalent bonds between the indicator and support materials prevents the indicator from leaching out and afforded electrospinable material for transformation into a nanofiber mat for direct solid phase measurement of nickel ions in water without further sample preparation. To obtain the optimal electrospinning conditions, several operational parameters were investigated including voltage, working distance and flow rate. Within the tested range (5–15 kV voltage, 10–20 cm working distance and 0.5–1.5 mL h^{-1} flow rate), the optimal spinning parameters which gave bead-free nanofibers prepared from 6.6 wt% solution are 8.75 kV voltage, 15 cm working distance and 1 mL h^{-1} flow rate (Fig. 3).

The fibers obtained were very soluble in water and even heating the fiber mat at 120 °C for 30 min did not affect solubility. Since their application was intended to be carried out in water samples, water solubility posed a challenge. Therefore there was the need to render these fibers water insoluble. In this regard, we employed the use of a cross-linker with the aim of forming a covalent bond. Cross-linking can be performed by chemical reactions that are initiated by heat, pressure, and change in pH or radiation. In this case, thermally cross-linkable β-cyclodextrin was chosen since it has free hydroxyl ends that are reactive and are capable of further esterification with the carboxylic acid groups on the product to form new ester bonds.[54] The cross-linked PAN–PAA electrospun fibers retained their fibrous structure after a long immersion in water.

The electrospun nanofiber PAN–PAA exhibited a distinct and well-defined emission peak as shown in Fig. 4. Previously, the intrinsic absorbance of PAN had been determined to be 470 nm.[30] However, the absorbance maximum of the new PAN-functionalized molecule was slightly red shifted to 479 nm. The emission maximum of the nanofiber mat was at 557 nm which is indicative of a good Stokes' shift. With the functionalization, the rate of self-quenching of PAN, as a result of site isolation, was greatly reduced. Consequently, the fluorescence efficiency and sensitivity of the nanofiber mat were remarkably improved.

Ni^{2+} response and selectivity of fluorescence PAN–PAA nanofiber

In order to get a clearer insight into the florescence of the nanofiber, the fluorescence behavior was evaluated after addition of various concentrations of Ni^{2+}. Fig. 5 shows the fluorescence "turn-off" effects of the nanofiber upon addition of Ni^{2+}. It was observed that addition of Ni^{2+} at low concentration of 0.1 μg mL^{-1} significantly decreased the emission intensity. When 1.0 μg mL^{-1} of Ni^{2+} was added, the fluorescence intensity decreased to less than 2%.

The sensitivity of the nanofiber was further visualized by fluorescence microscopy. After treating the nanofiber mat with

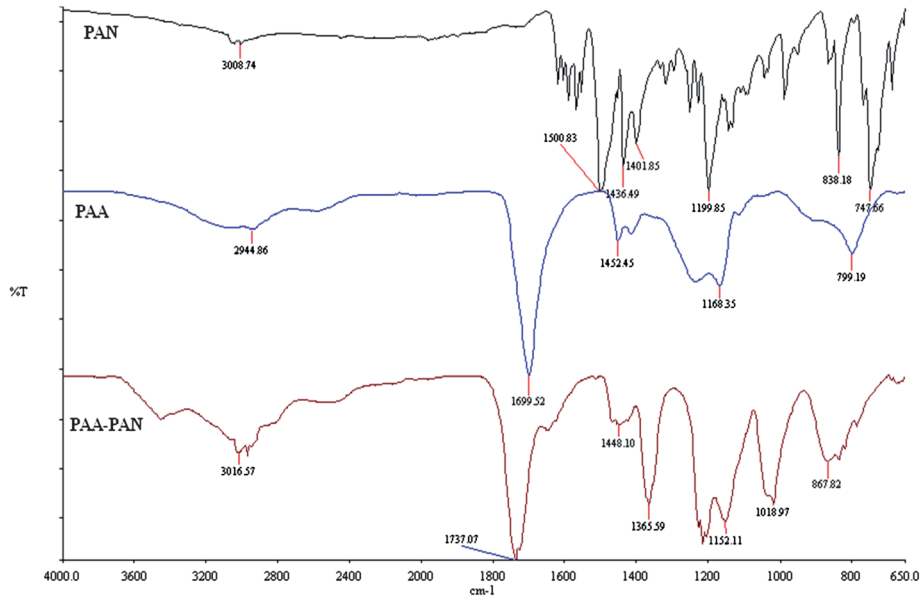

Fig. 2 FTIR spectra of new fluorescence polymer PAN–PAA, PAN and PAA.

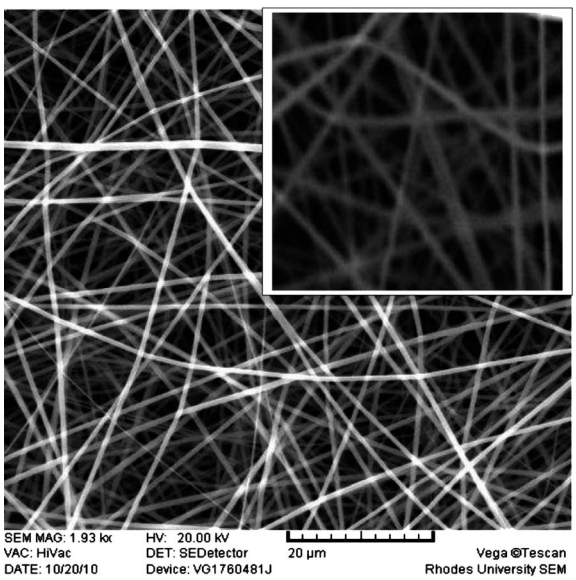

Fig. 3 SEM image of fluorescence functionalized electrospun PAA–PAN nanofibers (the inset shows the image of cross-linked fibers; the average fiber diameter range is 230–800 nm).

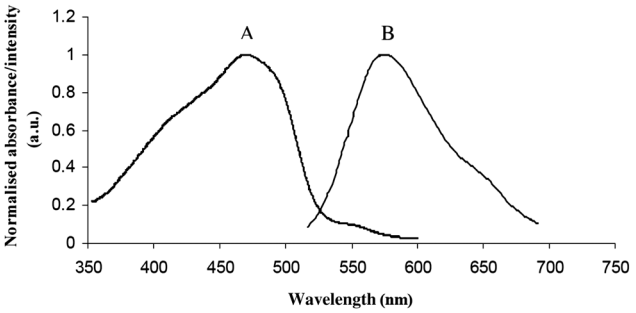

Fig. 4 UV absorption (A) and fluorescence emission (B) spectra of PAN–PAA nanofiber.

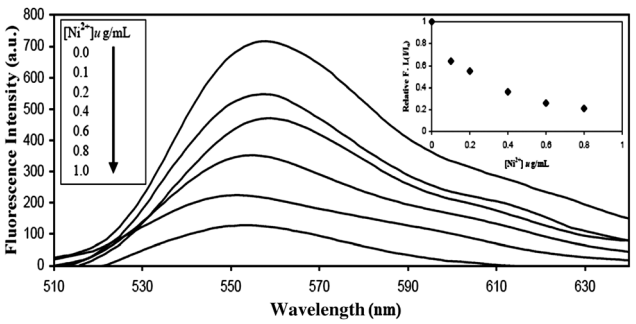

Fig. 5 Fluorescence emission spectra of PAN–PAA nanofiber as a function of Ni^{2+} concentration. The inset shows relative fluorescence intensities (I/I_0) at 557 nm with Ni^{2+} concentration.

a 1.0 μg mL^{-1} Ni^{2+} solution, remarkable quenching effects were observed from the fluorescence images (Fig. 6). Prior to the quenching processes, the fluorescence images evidently revealed fluorescence emission of the nanofiber and uniform dispersion of fluorophores. The sensitivity of the nanofiber could be restored by destabilizing the complex formed by rinsing with an acidic solution and this showed satisfactory reversibility and reproducibility of this system.

Fluorescence quenching by transition metal ions has been predominantly adduced to electron as well as energy transfer and paramagnetic interactions of the fluorophores and the metal ion.[55–57] Utilizing the Stern–Volmer mechanism (Fig. 7), the quenching of fluorescence by a metal ion may occur by at least two different mechanisms.[58] In the static quenching, on complexing of the ground state molecule with paramagnetic ion, fluorescence intensity decreases as a function of concentration of the metal ion introduced. However, a second mechanism must involve the excited state, rather than the ground state of the

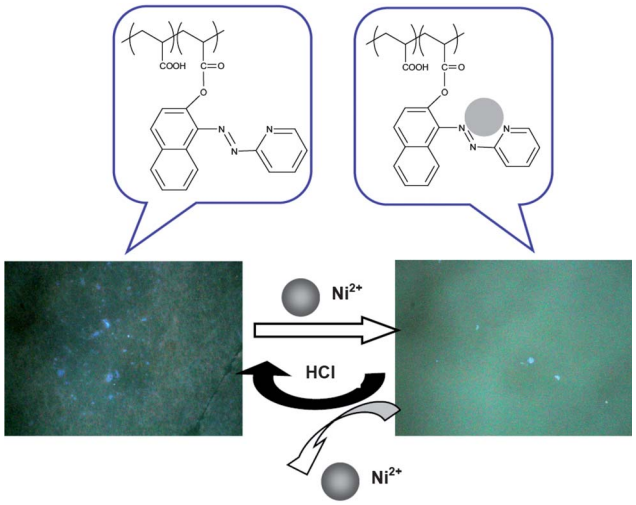

Fig. 6 Fluorescence images of sensing PAN–PAA nanofibers before and after immersion in a 1.0 μg mL^{-1} Ni^{2+} solution.

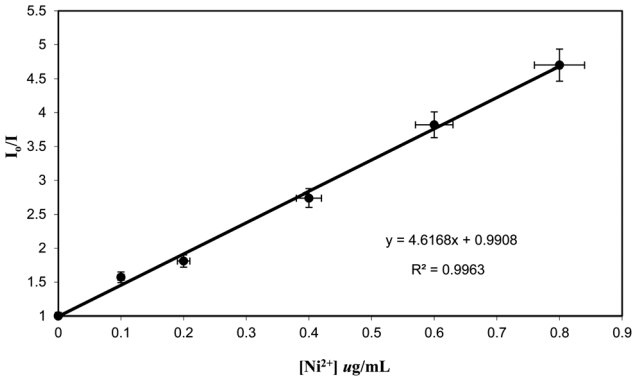

Fig. 7 A Stern-Volmer plot of fluorescence PAN–PAA nanofiber as a function of Ni^{2+} concentration.

fluorescent molecule. The paramagnetic metal ion causes a reduction of fluorescence intensity by inducing intersystem crossing. In an equilibrium situation, both of these effects may be operating and can be represented for the Ni–PAN–PAA system as shown (Scheme 2).

$(PAN–PAA)_o$, ^{1}(Ni-PAN–PAA) and ^{3}(Ni-PAN–PAA) are ground state fluorescence molecules, first excited singlet and triplet state respectively. The rationalization is that the rate of intersystem crossing (IC) in the first excited singlet complex is enhanced by the influence of the unpaired electrons of the nickel metal ion. The first excited singlet crosses over to the triplet state, which may then undergo some efficient type of quenching to return to the ground state.

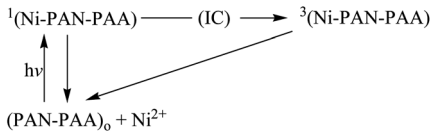

Scheme 2 Quenching mechanism of PAN–PAA by Ni^{2+}.

The relationship between the emission at 557 nm and Ni^{2+} concentrations can be deduced from the Stern–Volmer equation:

$$I_0/I = 1 + K_{sv}[Q] \quad (1)$$

where I_0 is the fluorescence intensity with the absence of quencher (Ni^{2+}), I is the intensity when the quencher is present, K_{sv} is the Stern–Volmer constant and [Q] is the concentration of quencher. The K_{sv} of the nanofiber, calculated from the slope of the plot was found to be 3.69×10^3 mL μg^{-1} indicative of enhanced sensitivity of the nanofiber probe that can be attributed to the higher surface area of the electrospun fiber. The linear range of the method lies between 0.1 and 1.0 μg mL^{-1} Ni^{2+}.

Table 1 gives the quality control parameters regarding the detection of nickel metal ions in aqueous solution. The accuracy of the determinations, expressed as relative error between the certified and the observed values of the reference material was ≤0.1%. The precision of these measurements expressed as relative standard deviation for eight repeated measurements of 1.0 μg mL^{-1} Ni^{2+} was also satisfactory, being lower than 4%. The limit of detection, based on the definition by IUPAC (LOD = 3δ/S)[59] was found to be 0.07 ng mL^{-1}. This LOD achieved with the PAN–PAA nanofibers was lower than 4.5 ng mL^{-1} achieved with a fluorescence-based sensor from *Escherichia coli* nickel binding protein labeled with *N*-[2-(1-maleimidyl)ethyl]-7-(diethylamino)coumarin-3-carboxamide.[60] In addition, the LOD is significantly lower than 0.04 μg mL^{-1} nickel concentrations above which it is toxic in drinking water as established by EPA.[61]

The selective binding ability of PAN–PAA nanofiber was determined as shown in Fig. 8. Given the quenching percentages of fluorescence intensity of PAN–PAA nanofiber, upon addition of 1.0 equiv. of various metal ions (Al^{3+}, Cr^{3+}, Fe^{2+}, Co^{2+}, Cu^{2+}, Zn^{2+}, Cd^{2+} and Pb^{2+}), obviously, PAN–PAA had a large chelation-enhanced quenching (CHEQ) effect only with Ni^{2+} among the metal ions examined with percentage quenching near 100%. In contrast, the addition of other metal ions (Al^{3+}, Cu^{2+}, Zn^{2+}, Cd^{2+} and Pb^{2+}) scarcely showed fluorescence quenching. However, Cr^{3+}, Fe^{2+} and Co^{2+} ions showed weak quenching probably due to their paramagnetic nature. Above all, this phenomenon indicated a high selectivity of PAN–PAA in its fluorescence quenching response toward Ni^{2+} against other metal ions.

The selectivity and tolerance of PAN–PAA for Ni^{2+} over other metal ions was examined by competition experiments. When 1 equiv. of Ni^{2+} in the presence of 10 equiv. of respective metal ion was introduced on the fiber, the emission spectra displayed a similar quenching near 557 nm to that of Ni^{2+} only. The results indicated that the fluorescence quenching by Ni^{2+} was hardly affected by the co-existence of other metal ions. When analyte solutions containing mixtures of competing species are used, the consideration of sensitivity and selectivity becomes more important. This result afforded a solid sensor for selective detection of nickel ion in water without laborious sample handling steps.

Another requirement for the solid detection sensors is its reusability. To investigate this ability, the nanofiber was used to complex Ni^{2+} through complex stripping cycles. The stripping agent used was 0.1 M HCl. Fig. 9 shows a profile of the

Table 1 Analytical quality control

I_0/I	Certified concentration (μg mL^{-1})	Concentration found (μg mL^{-1})	Relative error (%)	Relative standard deviation (%)	LOD (ng mL^{-1})	LOD[a] (ng mL^{-1})	LOD[b] (ng mL^{-1})
5.29	0.8980(0.0070)	0.8986(0.0040)	+0.0668	3.9203	0.0710	0.1	4.5

[a] Square-wave anodic stripping voltammetry bismuth-film electrode sensing method.[6] [b] Fluorescence-based sensing system using nickel binding protein from *Escherichia coli*.[60]

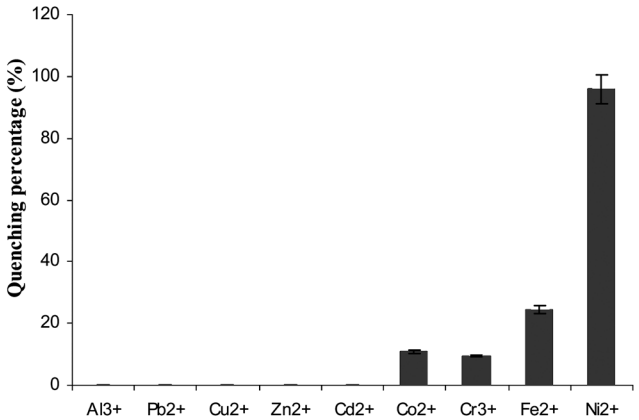

Fig. 8 Quenching percentage ($[I_0 - I/I_0] \times 100\%$) of fluorescence intensity of PAN–PAA nanofiber upon addition of 1.0 equiv. metal ions.

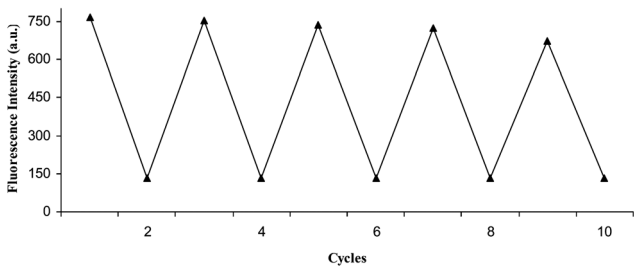

Fig. 9 Repeated switching of fluorescence emission of the PAN–PAA nanofiber against the number of Ni^{2+} solution/eluent cycles.

fluorescence response during five sequential cycles. The whole process included washing the fiber with HCl followed by modulating the pH value to neutral using 0.1 M NaOH and the sensing of Ni^{2+}. The nanofiber was found to be able to re-combine with Ni^{2+} at least four times ($I_4/I_1 = 94.8\%$) and the decrease of the fluorescence intensity may be attributed to the effect of stripping agents on the sensing performance and little loss of the fiber during multiple regeneration experiments.

The effect of the pH of the solution on the binding ability of PAN–PAA nanofiber with Ni^{2+} demonstrates that the functionalized polymer was disturbed by protons in the detection of metal ions. HCl was chosen as a simple stripping agent for the regeneration of nickel-free PAN–PAA nanofiber, because at pH below 5.0, the protonation of receptor nitrogen atoms of the PAN–PAA fiber decreases its electron donating abilities. However, at higher pH (>8.0) value, the precipitation of metal hydroxide which decomposes to the oxide is promoted.

Conclusions

A novel heterogeneous PAN–PAA nanofiber for selective detection of Ni^{2+} in water was developed successfully. The fabrication technique involved covalent functionalization of PAN on PAA polymer followed by electrospinning to produce a smooth and beadless fluorescence nanofiber. A Stern–Volmer bimolecular quenching relationship was found to hold when I_0/I was used to determine the analyte concentration. Importantly, the system showed high sensitivity in the range of concentration studied and also high selectivity in its fluorescence "turn-off" response toward Ni^{2+} against other metal ions. Further, a reversible process can be realized by breaking of indicator–quencher complexation and fluorescence "turn-on", allowing reusability for at least four cycles. The approach may serve as a foundation for the preparation of a practical fluorescent detector for potential practical applications. Further work in this regard is in progress in our laboratory. We hope that this work will contribute to the development of the versatile technique of electrospinning for fabrication of fluorescence nanofiber with application in both environmental and biological systems.

Acknowledgements

The authors acknowledge Water Research Commission (WRC) South Africa, African Network of Analytical Chemists (SEA-NAC), Rhodes University and the National Research Foundation (NRF) for the funding.

References

1 K. Rurack, *Spectrochim. Acta, Part A*, 2001, **57**, 105–113.
2 A. Sigel, H. Sigel, and R. K. O. Sigel, *Nickel and its Surprising Impact in Nature*, John Wiley & Sons Ltd, U.K., 2007.
3 J. E. R. Goodman, L. Prueitt, D. G. Dodge and S. Thakali, *Crit. Rev. Toxicol.*, 2009, **39**, 365–417.
4 M. Costa, T. L. Davidson, H. Chen, Q. Ke, P. Zhang, Y. Yan, C. Huang and T. Kluz, *Mutat. Res.*, 2005, **592**, 79–88.
5 A. A. Nemec, G. D. Leikauf, B. R. Pitt, K. Wasserloos and J. A. Barchowsky, *Am. J. Respir. Cell Mol. Biol.*, 2009, **41**, 69–75.
6 C. Kokkinos, A. Economou, I. Raptis and T. Speliotis, *Anal. Chim. Acta*, 2008, **622**, 111–118.
7 E. A. Takara, S. D. Pasini-Cabello, S. Cerutti, J. A. Gasquez and L. D. J. Martinez, *J. Pharm. Biomed. Anal.*, 2005, **39**, 735–739.
8 M. A. Bezerra, W. N. L. dos Santos, V. A. Lemos, M. Korn and S. L. C. Ferreira, *J. Hazard. Mater.*, 2007, **148**, 334–339.
9 K. Jankowski, J. Yao, K. Kasiura, A. Jackowska and A. Sieradzka, *Spectrochim. Acta, Part B*, 2005, **60**, 369–375.
10 D. Zendelovska, G. Pavlovska, K. Cundeva and T. Stafilov, *Talanta*, 2001, **54**, 139–146.
11 T. Stafilov, *Spectrochim. Acta, Part B*, 2000, **55**, 893–906.
12 J. Shiowatana, K. Benyatianb and A. Siripinyanond, *Spectrochim. Acta, Part B*, 2000, **21**, 179–185.
13 A. U. Karatepe, M. Soylak and L. Elci, *Anal. Lett.*, 2003, **36**, 797–812.

14 L. Elci, M. Soylak and B. Ozcan, *Anal. Lett.*, 2003, **36**, 987–999.
15 Q. M. Li, X. H. Zhao, K. Jiang and G. G. Liu, *Chin. Sci. Bull.*, 2007, **52**, 65–70.
16 T. Kiriyama and R. Kuroda, *Fresenius' J. Anal. Chem.*, 1988, **332**, 338–340.
17 P. S. Tonello, A. H. Rosa, C. H. Abreu and A. A. Menegario, *Anal. Chim. Acta*, 2007, **598**, 162–168.
18 J. Yao, W. Dou, W. Qin and W. Liu, *Inorg. Chem. Commun.*, 2009, **12**, 116–118.
19 Y. Wang, G. Qian, Z. Xiao, H. Wang, L. Long, H. Wang, Z. Li and X. Liu, *Inorg. Chim. Acta*, 2010, **363**, 2325–2332.
20 T. Cheng, Y. Xu, S. Zhang, W. Zhu, X. Qian and L. Duan, *J. Am. Chem. Soc.*, 2008, **130**, 16160–16161.
21 S. C. Dodani, Q. He and C. J. Chang, *J. Am. Chem. Soc.*, 2009, **131**, 18020–18021.
22 L.-J. Fan and W. E. Jones Jr, *J. Am. Chem. Soc.*, 2006, **128**, 6784–6785.
23 K. Ogawa, F. Guo and K. S. Schanze, *J. Photochem. Photobiol., A*, 2009, **207**, 79–85.
24 T. Moriuchi-Kawakami, Y. Hisada and Y. Shibutani, *Chem. Cent. J.*, 2010, **4**(7), 1–9.
25 S.-H. Lee, J. Kumar and S. K. Tripathy, *Langmuir*, 2000, **16**, 10482–10489.
26 G. F. Farruggia, S. Lotti, L. Prodi, M. Montalti, N. Zaccheroni, P. B. Savage, V. Trapani, P. Sale and F. I. Wolf, *J. Am. Chem. Soc.*, 2006, **128**, 344–350.
27 X. Peng, J. Du, J. Fan, J. Wang, Y. Wu, J. Zhao, S. And Sun and T. Xu, *J. Am. Chem. Soc.*, 2007, **128**, 1500–1501.
28 X. Qi, E. J. Jun, L. Xu, S.-J. Kim, J. S. Joong Hong, Y. J. Yoon and J. Yoon, *J. Org. Chem.*, 2006, **71**, 2881–2884.
29 R. G. Pearson, *J. Am. Chem. Soc.*, 1963, **85**, 3533–3539.
30 N. A. Gavrilenko and N. V. Saranchina, *J. Anal. Chem.*, 2009, **64**(3), 226–230.
31 T. E. Brook and R. Narayanaswamy, *Sens. Actuators, B*, 1998, **51**, 77–83.
32 M. P. Xavier, D. Garcia-Fresnadillo, M. C. Moreno-Bondi and G. Orellana, *Anal. Chem.*, 1998, **70**, 5184–5189.
33 X. Wang, C. Drew, S.-H. Lee, K. J. Senecal, J. Kumar and L. A. Samuelson, *Nano Lett.*, 2002, **2**(11), 1273–1275.
34 D. H. Reneker and I. Chun, *Nanotechnology*, 1996, **7**, 216–223.
35 C. He, W. Zhu, Y. Xu, T. Chen and X. Qian, *Anal. Chim. Acta*, 2009, **651**, 227–233.
36 T. Balaji, S. A. El-Safty, H. Matsunaga, T. Hanaoka and F. Mizukami, *Angew. Chem., Int. Ed.*, 2006, **45**, 7202–7208.
37 S. Shin and J. Jang, *Chem. Commun.*, 2007, 4230–4232.
38 L. Gao, J. Q. Wang, L. Huang, X. X. Fan, J. H. Zhu, Y. Wang and Z. G. Zou, *Inorg. Chem.*, 2007, **46**, 10287–10293.
39 L. Gao, Y. Wang, J. Wang, L. Huang, L. Shi, X. Fan, Z. Zou, T. Yu, M. Zhu and Z. Li, *Inorg. Chem.*, 2006, **45**, 6844–6850.
40 K. Kledzik, M. Orłowska, D. Patralska, M. Gwiazda, J. Jezierska, S. Pikus, R. Ostaszewski and A. M. Kłonkowski, *Appl. Surf. Sci.*, 2007, **254**, 441–451.
41 S. J. Lee, D. R. Bae, W. S. Han, S. S. Lee and J. H. Jung, *Eur. J. Inorg. Chem.*, 2008, **10**, 1559–1564.
42 K. Sarkar, K. Dhara, M. Nandi, P. Roy, A. Bhaumik and P. Banerjee, *Adv. Funct. Mater.*, 2009, **19**, 223–234.
43 M. J. Ruedas-Rama and E. A. H. Hall, *Anal. Chem.*, 2008, **80**, 8260–8268.
44 J. N. Demas, B. A. DeGraff and W. Xu, *Anal. Chem.*, 1995, **67**, 1377–1380.
45 E. R. Carraway, J. N. Demas and B. A. DeGraff, *Langmuir*, 1991, **7**, 2991–2998.
46 W. Xu, K. A. Kneas, J. N. Demas and B. A. DeGraff, *Anal. Chem.*, 1996, **68**, 2605–2609.
47 I. Klimant and O. S. Wolfbeis, *Anal. Chem.*, 1995, **67**, 3160–3166.
48 A. Mills, A. Lepre, B. R. Theobald, E. Slade and B. A. Murrer, *Anal. Chem.*, 1997, **69**, 2842–2847.
49 G. Di Marco, M. Lanza and S. Campagna, *Adv. Mater.*, 1995, **7**, 468–471.
50 C. McDonagh, B. D. MacCraith and A. K. McEvoy, *Anal. Chem.*, 1998, **70**, 45–50.
51 Z. Zhujun and W. R. Seitz, *Anal. Chim. Acta*, 1984, **160**, 47–55.
52 Z. Zhujun, Y. Zhang, M. Wangbai, R. Russell, Z. M. Shakhsher, C. L. Grant and W. R. Seitz, *Anal. Chem.*, 1989, **61**, 202–205.
53 A. Lobnik, I. Oehme, I. Murkovic and O. S. Wolfbeis, *Anal. Chim. Acta*, 1998, **367**, 159–165.
54 M. Ziabari, V. Mottaghitalab and A. K. Haghi, *Braz. J. Chem. Eng.*, 2008, **26**, 53–62.
55 A. W. Varnes, R. B. Dodson and E. L. Wehry, *J. Am. Chem. Soc.*, 1972, **94**, 946–951.
56 J. A. Kelmo and T. M. Shepherd, *Chem. Phys. Lett.*, 1977, **47**, 158–162.
57 S. J. Formosinho, *Mol. Photochem.*, 1976, **7**, 13–39.
58 J. R. Lakowicz, *Principles of Fluorescence Spectroscopy*, Plenum Press, New York, 1983.
59 H. M. N. H. Irving, H. Freiser and T. S. West, *IUPAC Compendium of Analytical Nomenclature, Definitive Rules*, Pergamon Press, Oxford, 1981.
60 L. L. E. Salins, E. S. Goldsmith, C. M. Ensor, S. Daunert, Z. M. Shakhsher, C. L. Grant and W. R. Seitz, *Anal. Bioanal. Chem.*, 2002, **372**, 174–180.
61 Agency for Toxic Substances and Disease Registry (ATSDR), *Toxicological Profile for Nickel (Update)*, U.S. Department of Public Health and Human Services, Public Health Service, Atlanta, GA, 2005.